Original Article
Cistanche phenylethanoid glycosides induce apoptosis and pyroptosis in T-cell lymphoma

Ying Tang[1,2*], Fangxin Zhao[1,2*], Xuan Zhang[2], Yan Niu[2], Xiulan Liu[2], Renqiqige Bu[2], Yunlong Ma[3], Geyemuri Wu[2], Beibei Li[2], Hongxin Yang[2], Jianqiang Wu[1,2]

*[1]School of Life Sciences, Inner Mongolia University, Hohhot, Inner Mongolia, China; [2]College of Basic Medicine, Inner Mongolia Medical University, Hohhot, Inner Mongolia, China; [3]School of Life Sciences, Inner Mongolia Agricultural University, Hohhot, Inner Mongolia, China. *Equal contributors.*

Abstract: *Cistanche deserticola*, known for its extensive history in Traditional Chinese Medicine (TCM), is valued for its therapeutic properties. Recent studies have identified its anticancer capabilities, yet the mechanisms underlying these properties remain to be fully elucidated. In this study, we determined that a mixture of four cistanche-derived phenylethanoid glycosides (CPhGs), echinacoside, acteoside, 2-acetylacteoside, and cistanoside A, which are among the main bioactive compounds in *C. deserticola*, eliminated T-cell lymphoma (TCL) cells by inducing apoptosis and pyroptosis *in vitro* and attenuated tumor growth *in vivo* in a xenograft mouse model. At the molecular level, these CPhGs elevated P53 by inhibiting the SIRT2-MDM2/P300 and PI3K/AKT carcinogenic axes and activating PTEN-Bax tumor-suppressing signaling. Moreover, CPhGs activated noncanonical and alternative pathways to trigger pyroptosis. Interestingly, CPhGs did not activate canonical NLRP3-caspase-1 pyroptotic signaling pathway; instead, CPhGs suppressed the inflammasome factor NLRP3 and the maturation of IL-1β. Treatment with a caspase-1/4 inhibitor and silencing of Gasdermin D (GSDMD) or Gasdermin E (GSDME) partially rescued CPhG-induced cell death. Conversely, forced expression of NLRP3 restored cell proliferation. In summary, our results indicate that CPhGs modulate multiple signaling pathways to achieve their anticancer properties and perform dual roles in pyroptosis and NLRP3-driven proliferation. This study offers experimental support for the potential application of CPhGs in the treatment of TCL.

Keywords: Cistanche phenylethanoid glycosides, apoptosis, pyroptosis, NLRP3

Introduction

T-cell lymphoma (TCL) represents a spectrum of malignancies classified under non-Hodgkin lymphoma. While some TCL variants show slow progression and respond well to treatment, others exhibit resistance to current therapeutic strategies. In consideration of developing new pharmaceutical agents for cancers, the active ingredients of Traditional Chinese Medicine (TCM) have garnered increasing attention [1]. *Cistanche deserticola*, a member of the *Cistanche* genus which predominantly includes *Cistanche deserticola* and *Cistanche tubulosa*, is recognized as an authentic herb in TCM, with a lengthy history of application in various formulations aimed at treating a broad spectrum of diseases, including cancer [2, 3]. Extensive research has confirmed the safety of *Cistanche* species for human consumption at typical doses in TCM formulation [3, 4]. Cistanche-derived phenylethanoid are the primary bioactive components of *cistanche* varieties. The four main bioactive ingredients in *C. deserticola* comprise echinacoside, acteoside, 2-Acetylacteoside, and cistanoside A, accounting for approximately 0.22-0.85%, 0.04%-0.93%, 0.05-0.63%, and 0.04-0.13% of the total weights of the dried whole herb, respectively [5, 6]. Studies have shown that individual or mixtures of Cistanche-derived phenylethanoid glycosides have anti-tumor activities, in addition to their anti-inflammatory, anti-aging, anti-fatigue, liver-protective, and immunomodulatory properties [7-9]. Whole extracts of *C. deserticola* or its purified phenylethanoid glycosides have been found to inhibit various types of cancers such as breast, ovarian, hepatocellular, glioblasto-

ma, and pancreatic cancers, both *in vitro* and *in vivo* by influencing cellular signaling, including Wnt/β catenin, PI3K/AKT, miR-503-3p, and SKP2 [10-15].

Phenylethanoid glycosides have been shown to induce apoptosis in several cancer models [8, 14, 16]. Recent studies have also indicated that the role of pyroptosis, an inflammatory signal-mediated cell death, in the action of phenylethanoid glycosides [17]. Induction of pyroptosis, with or without apoptosis, represents a crucial strategy for eliminating cancer cells [18]. In TCL, the involvement of critical pro-apoptotic and anti-apoptotic proteins, including P53, PTEN, SIRT2, and PI3K/AKT, in apoptosis or pyroptosis induced by phenylethanoid glycosides, and the activation of pyroptosis, remain underexplored.

In this study, we explored a mixture of the four most prevalent phenylethanoid glycosides, echinacoside, acteoside, 2-acetylacteoside, and cistanoside A (referred to as CPhGs), to study the synergistic tumor-suppressing effects of TCM on TCL. We discovered that CPhGs significantly killed and inhibited TCL *in vitro* and *in vivo*. Our study found that CPhGs predominantly induce cell death in T lymphoma cells through apoptosis and pyroptosis, via the regulation of multiple interconnected pathways involving key proteins such as P53 and caspase-3. Moreover, we also identified a novel mechanism by which CPhGs suppress NLRP3 inflammatory signaling while activating pyroptosis and apoptosis, thus maximizing their anticancer effect in TCL.

Materials and methods

Cell lines and reagents

Human TCL lines Jurkat (ATCC), HH, Hut-78 (ATCC), and MyLa (Sigma-Aldrich) were cultured as described previously [19, 20]. All cell lines were authenticated by short tandem repeat (STR) markers, and tested for mycobacterial contamination by mycoplasma agar culture. Echinacoside, Acteoside, Cistanoside A, and 2-Acetylacteoside (> 98% purity for all) were purchased from Yuanye Bio-Technology (Shanghai, China), and used as an equal concentration mixture (CPhGs), as indicated in the experiments. Specific inhibitors Z-VAD-FMK (Z-VAD) and VX765 were purchased from Selleckchem (Houston, TX).

Proliferation assays and apoptosis assays

Proliferation assays were performed using a CCK-8 kit from Meilunbio (Dalian, China). Briefly, cells were cultured and then treated with indicated concentrations of CPhGs, with or without inhibitors, for 3 days before the addition of CCK-8 solution, and absorbance was measured following the manufacturer's instructions. For apoptosis analysis, cells were treated with CPhGs at indicated concentrations for 48 h. An Annexin V apoptosis detection kit and flow Flowcytometry were utilized for staining and detection, respectively, with FlowJo software used for data analysis.

GSDMD and GSDME knockdown

GSDMD and GSDME knockdown was achieved using siRNA. siRNA oligos targeting GSDMD (#SR312602), GSDME (#SR301192), or non-specific siRNAs were purchased from OriGene (Rockville, MD). Cells were transfected with siRNAs through electroporation using an Amaxa Nucleofector II Device from Lonza (Basel, Switzerland). Briefly, 1×10^6 cells were centrifuged and resuspended in 100 µl of transfection solution L, and siRNA was added to a final concentration of 1 mM. Transfection was carried out using the Nucleofector program X-001. Cells were then cultured for 24 h before further experimentation.

Expressing plasmid vector construction and transfection

The NLRP3 gene (cDNA) was reverse-transcribed from mRNA, PCR-amplified, purified, and inserted into the pcDNA3.1-GFP plasmid. Following clone selection in *Escherichia coli* bacterial and Ampicillin screening, the insert was confirmed by sequencing. The plasmid DNA was then extracted, purified, and transfected into cells through electroporation using a Nucleofector. Transfection efficiency was assessed by detecting GFP expression using flow Flowcytometry, and transfected cells were used for functional assays.

Western blotting

Cells were washed with PBS, collected, and lysed for total protein extraction. Proteins were then resolved by SDS-PAGE, transferred to membranes, and probed with primary and secondary antibodies. Detection was perfor-

med using a Meilunbio enhanced chemiluminescence kit (Dalian, China). Antibodies against P300, Bcl-2, BAX, AKT, p-AKT, PTEN, caspase-3, cleaved caspase-3, caspase-8, cleaved caspase-8, caspase-9, cleaved caspase 9, GSDMD, and GAPDH were obtained from Cell Signaling (Boston, MA); SIRT2, MDM2, and P53 antibodies were from Abclonal (Woburn, MA), caspase-1, GSDME, and ASC antibodies were obtained from Abcam (Waltham, MA); PI3K, p-PI3K, and NLRP3 antibodies were obtained from GeneTex (Irvine, CA).

LDH activity assay

Cells were treated with CPhGs for 48 h (pretreated with 20 µM VX765 for 1 h for rescue assays) followed by supernatant collection. LDH levels were determined using an LDH assay kit from Jiancheng Biotechnology (Nanjing, China) according to the manufacturer's instructions.

In vivo studies

Mouse studies were approved by the Laboratory Animal Ethics Committee of Inner Mongolia Medical University (Hohhot, China) and conducted in accordance with the European Community guidelines for laboratory animal use and care. To establish xenograft tumors, Hut78 cells (1×10^7) were resuspended in 100 µL of 1640 medium, and injected subcutaneously into the right flank of BALB/c nude mice (n=6/group). Six days after injection, mice bearing xenograft TCL were treated with saline or different doses of CPhGs (20 or 60 mg/kg) through intraperitoneal injection for 12 days. Tumor growth was monitored every 3 days for 18 days. Mice were then euthanized, and tumor samples were collected for further analysis.

Histology

For hematoxylin and eosin (H&E) and immunohistochemical staining, tumor samples were fixed in 4% formaldehyde, embedded in paraffin, and sectioned at 4-5 µm thickness for staining. Images were captured using a microscope and analyzed quantitatively with Image-Pro Plus 6.0 software (Rockville, MD).

Statistical analysis

Statistical differences between cell treatment and control groups *in vitro* were analyzed using Student's t-test. Experiments were conducted in triplicate. Data are presented as mean ± SD, with statistical significance defined at $P < 0.05$.

Results

CPhGs induced cell death, inhibited cell proliferation, and triggered intrinsic and extrinsic apoptosis in TCL

Initially, to explore the cytotoxic effects of CPhGs, we treated the TCL cell lines HH, Hut78, MyLa, and Jurkat with various concentrations of CPhGs for 3 d and assessed live/dead rates using the Cell-Counting Kit-8 (CCK-8) cell viability assay. Treatment with CPhGs resulted in dose-dependent cell death (**Figure 1A**) and significantly reduced proliferation at concentrations of 40 µM and 80 µM compared to the control group (**Figure 1B**). Since anticancer drugs can induce various types of cell death, with apoptosis being the most common form of programmed cell death, we subsequently investigated whether CPhGs prompted apoptosis via Annexin V/PI staining and flow Flowcytometry analysis. CPhGs induced significant and dose-dependent apoptosis in all four cell lines (**Figure 1C** and **1D**). In addition, in the TCL mouse model, the number of dead cells was significantly increased in the tumor tissues of the CPhGs-treated group juxtaposed with the control group (**Figure 1E**). Moreover, the activation of intrinsic and extrinsic apoptosis markers, caspase-9, caspase-8, and the apoptosis executor, caspase-3 (**Figure 2**) suggested the activation of both intrinsic and extrinsic apoptotic pathways.

CPhGs induced pyroptosis via non-canonical and alternative pyroptotic pathways

Given evidence that phenylethanoid glycosides may induce pyroptosis, we explored whether CPhGs triggered pyroptosis in HH and Hut78 cells. CPhGs facilitated the cleavage of GSDMD, a marker of the non-canonical pyroptotic pathway, and GSDME, a marker of an alternative pyroptotic pathway marker (**Figure 3A**). Lactate dehydrogenase (LDH) is a cytosolic enzyme typically retained within the cell cytosol, is released upon loss of membrane integrity. To further validate CPhGs-induced pyroptosis in TCL cells, we measured LDH levels in cell culture supernatants before and after treatment, observing elevated LDH levels following CPhGs
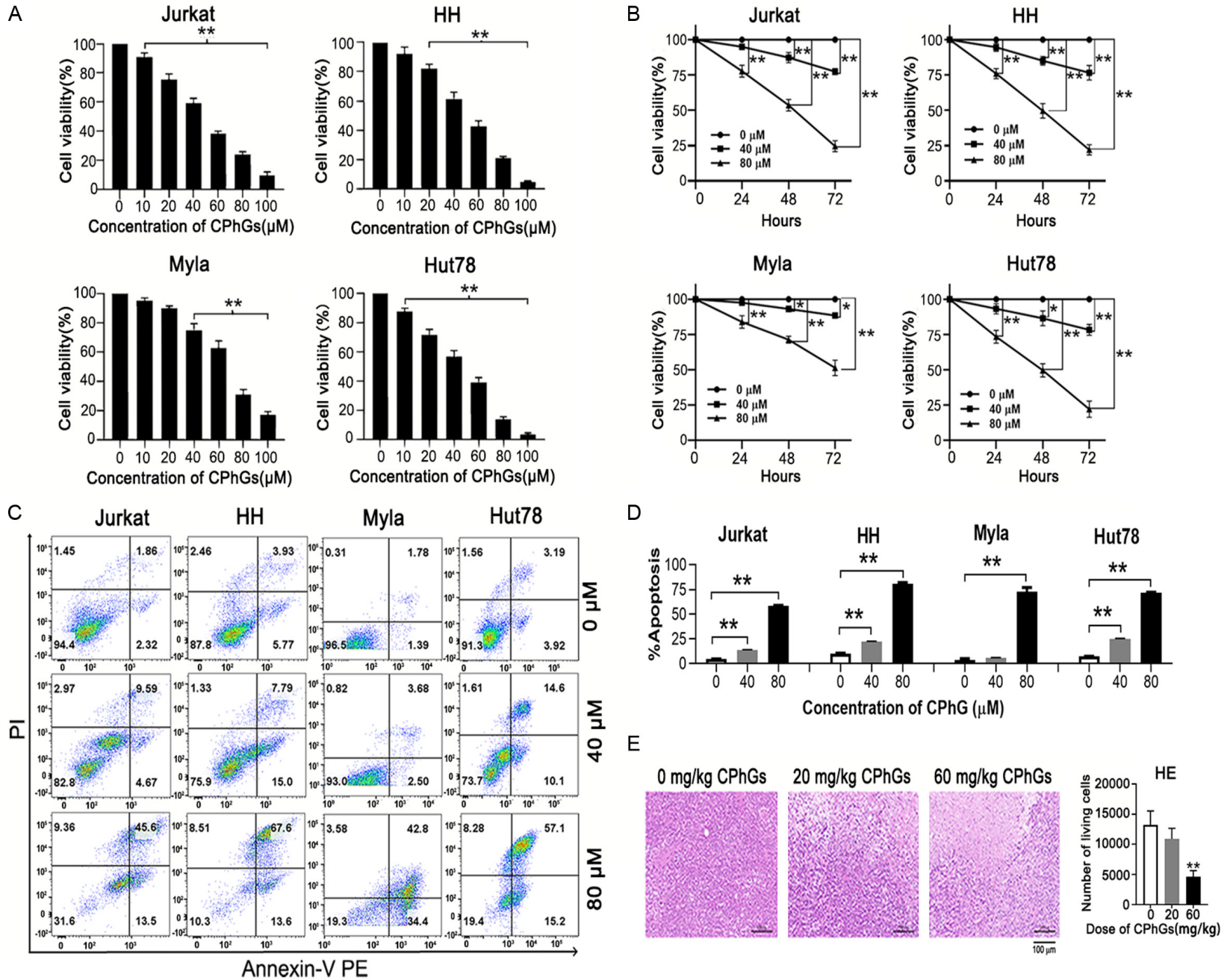
Figure 1. CPhGs inhibited cell proliferation and triggered apoptosis in TCL. Cell lines HH, Hut78, Myla, and Jurkat were treated with different concentrations of CPhGs. A. Changes in the percentage of living cells as measured by CCK8 assay. B. Cell growth curves of the four cell lines treated with CPhGs over 3 d. C. Representative flow cytometry analysis of four cell lines treated with indicated concentrations of CPhGs for 48 h. D. Quantitative analysis of apoptosis detected by Annexin V/PI staining and flow cytometry. E. Representative images of H&E staining of xenograft tumor tissues of mice treated with indicated doses of CPhGs (left) and quantification of living cells (right). Data are presented as mean ± SD. *P < 0.05, **P < 0.01. Scale: 100 µm.
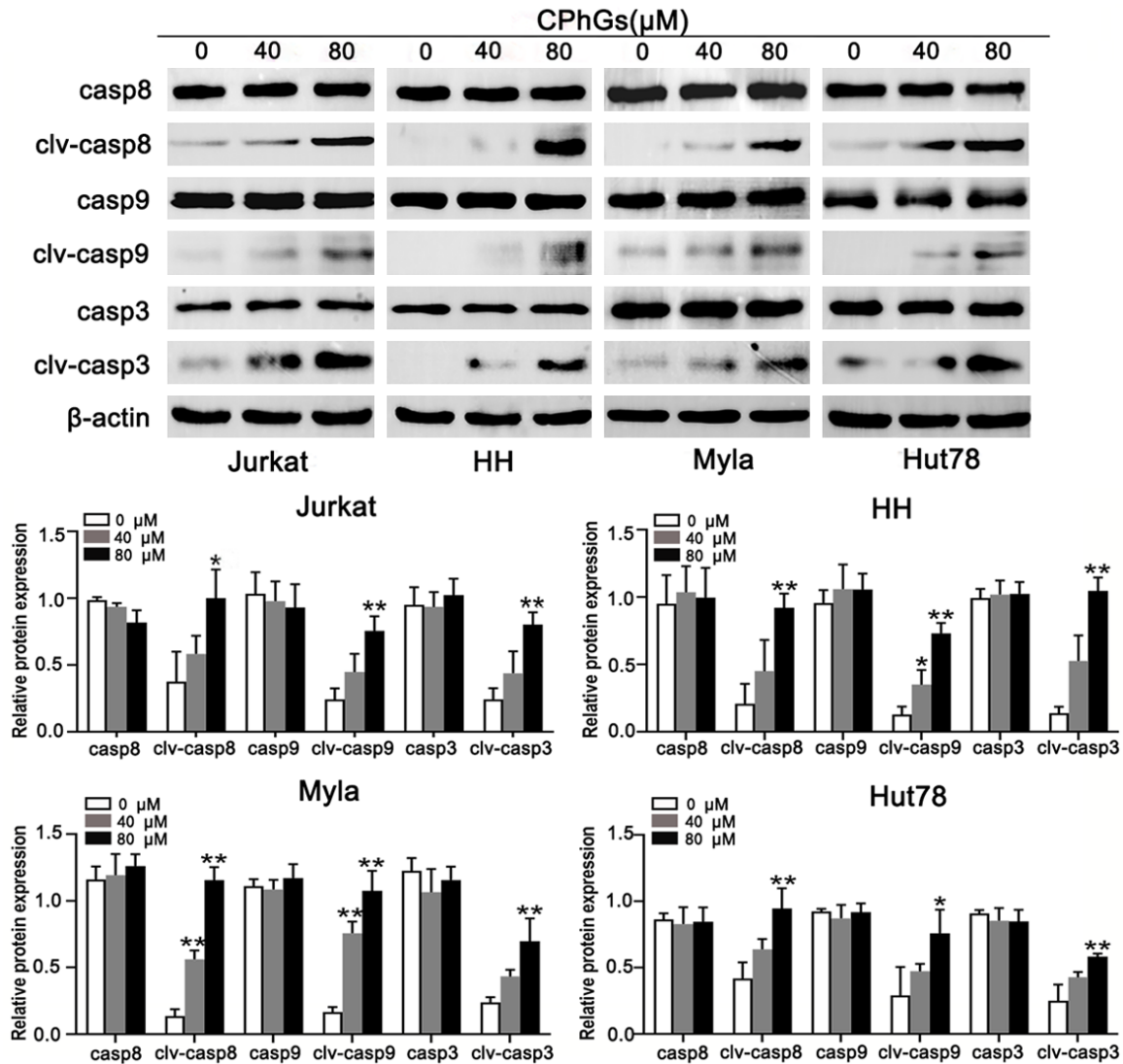
Figure 2. CPhGs activated both intrinsic and extrinsic apoptotic pathways. The intrinsic pathway marker cleaved caspase-9, the extrinsic marker cleaved caspase-8, and the apoptosis executor cleaved caspase-3 were detected by Western blotting (upper) and quantified (lower). Data are represented as the mean ± SD. Results are from three individual replicates. One-way ANOVA was used for statistical analysis. *P < 0.05, **P < 0.01 vs. the control groups.

treatment (**Figure 3B**). Despite GSDMD serving as a shared executor of both canonical and non-canonical pyroptotic pathways, the canonical pathway appeared inactive in CPhGs-treated cells, as evidenced by the absence of cleaved caspase-1, even though caspase-4, a marker of the non-canonical pyroptotic path-

way, was cleaved (**Figure 3C**). These findings suggest that the activation of non-canonical and alternative signaling pathways is responsible for CPhGs-induced pyroptosis in TCL cells.

As pyroptosis is mediated by caspase-4, we investigated the rescue effects of the cas-
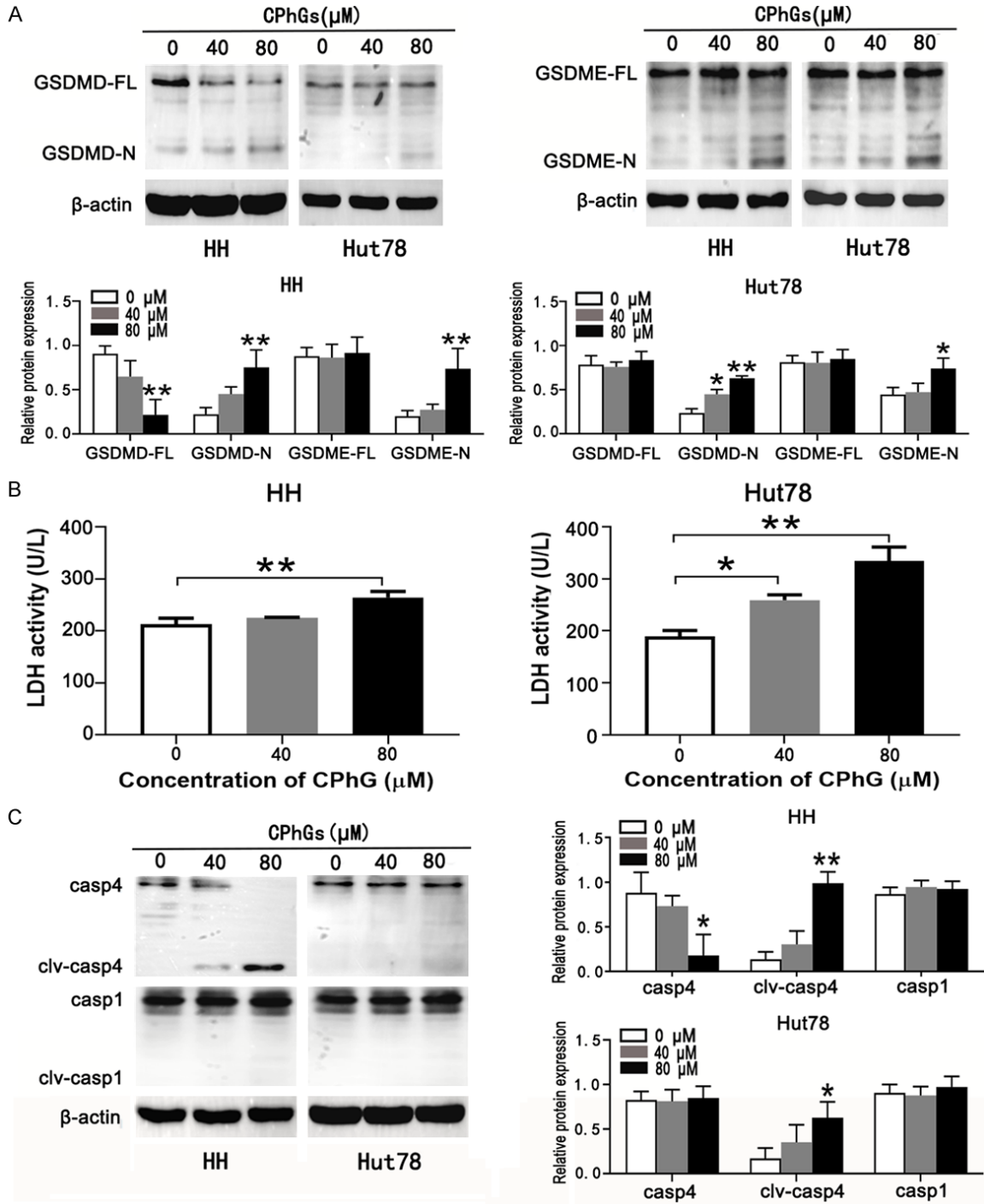
Figure 3. CPhGs induced pyroptosis. HH and Hut78 cells were treated with indicated concentrations of CPhGs. A. Western blotting of cleaved GSDMD and GSDME (upper) with quantitative analysis (lower). B. Changes in LDH levels. C. Western blotting analysis of cleaved caspase-4 and caspase-1 (left) and the quantitative analysis (right).

pase-4 inhibitor VX765 after CPhGs treatment along with the apoptosis inhibitor ZVAD-FMK (ZVAD) to examine changes in pyroptosis and apoptosis ratios. HH and Hut78 cells were treated with CPhGs alone, in combination with VX765, ZVAD, or VX765 plus ZVAD. Both VX765 and ZVAD significantly decreased CPhGs-induced cell death, with ZVAD exhibiting a greater reduction than VX765. The percentage of viable cells increased from 52% to 74% and

58% to 78% in HH and Hut78, respectively, after co-treatment with CPhGs and VX765, whereas co-treatment with CPhGs and ZVAD increased the percentage of living cells from 52% to 82% and 58% to 80% in the same cell lines. Combined treatment with VX765 and ZVAD completely blocked cell death induced by CPhGs (**Figure 4A**). Treatment with VX765 partially blocked CPhGs-induced LDH release and caspase-4 cleavage or activation (**Figure 4B** and **4C**). To further confirm that pyroptosis is a mechanism through which CPhGs induce cell death in malignant T cells, we determined the role of pyroptosis executors, GSDMD and GSDME, in CPhGs-induced killing of TCL through siRNA silencing. As hypothesized, silencing GSDMD and GSDME partially rescued cell viability (**Figure 4D**).

CPhGs inhibited NLRP3 expression and IL-1β maturation

Given that CPhGs did not induce caspase-1 activation, we explored whether other factors in the canonical pyroptotic pathway were activated. Interestingly, the expression of NLRP3, an initiating factor of the NLRP3 inflammasome complex, was down-regulated after CPhGs treatment (**Figure 5A**). As NLRP3 inflammasome signaling facilitates both canonical pyroptosis and IL-1β-dependent proliferation, we speculate that CPhGs not only fail to activate the canonical pyroptosis pathway but also actively suppress proliferation signaling. Consequently, we assessed IL-1β levels before and after CPhGs treatment in HH and Hut78 cells. The protein level of IL-1β decreased proportionally with NLRP3 downregulation in a dose-dependent manner following CPhGs treatment (**Figure 5A**). Similarly, *in situ* immunohistochemical staining of tumor tissue sections from the TCL xenograft mouse model also displayed reduced NLRP3 expression after CPhGs treatment juxtaposed with the control (**Figure 5B**). To further confirm the role of NLRP3 in cell proliferation, we induced exogenous NLRP3 expression by plasmid transfection into HH and Hut78 cells pre-treated with CPhGs, resulting in a partial restoration of proliferation in both CPhGs-treated cell lines (**Figure 5C**).

CPhGs regulates SIRT2-MDM2/P300 and PI3K/AKT pathways

P53, a crucial tumor suppressor, is inhibited by the SIRT2-P300/MDM2 signaling axis. The PI3K/AKT pathway promotes proliferation and is involved in the carcinogenesis of various cancer types. To further investigate the influence of CPhGs on the major pathways influencing cancer development, we examined SIRT2/P53, PI3K/AKT, and other pro- and anti-apoptotic signaling pathways. As shown in **Figure 6**, CPhGs treatment significantly reduced the expression of SIRT2, P300, MDM2, and Bcl2; inhibited PI3K and AKT activation; and upregulated P53, PTEN, and BAX expression in a dose-dependent manner, as compared to controls. *In situ* immunohistochemical staining of tumor tissues from the TCL xenograft mouse model also indicated increased expression of P53 after CPhGs treatment (**Figure 6A-D**).

CPhGs inhibited TCL tumor growth in xenograft mouse model

*T*o investigate the effects of CPhGs on TCL tumor growth in *vivo*, we established a xenograft TCL tumor model. Tumor cells were subcutaneously injected into BALB/c female nude mice (6-8 weeks old). Mice bearing TCL cell-derived tumors were then intraperitoneally injected with saline, 20 mg/kg CPhGs, or 60 mg/kg CPhGs. Tumors were surgically removed after 12 days of continuous dosing. CPhGs significantly inhibited tumor growth in a dose-dependent manner (**Figure 7A**). Tumor growth curves, where tumor volumes measured every 3 days, were plotted (**Figure 7B**), and showed an increase in the body weight of mice treated with CPhGs (**Figure 7C**), indicating that CPhGs were well-tolerated at the administered doses, and might even improve the physical conditions of tumor-bearing mice. The tumor inhibition rates on day 18 were also calculated (**Figure 7D**).

Discussion

The efficacy of TCM relies on the combined functions of many compounds. It has the advantage of additive or synergistic effects; however, this complexity also poses challenges for analyzing the functions of each compound individually. One practical method is to use a few of the main bioactive ingredients of one herb or formula as the study target to obtain the most representative data [21]. In this study, we used a mixture of the four most abundant CPhGs in *C. deserticola* to replicate the natural synergistic effects of CPhGs observed in TCM formulas incorporating *C. deserticola*.
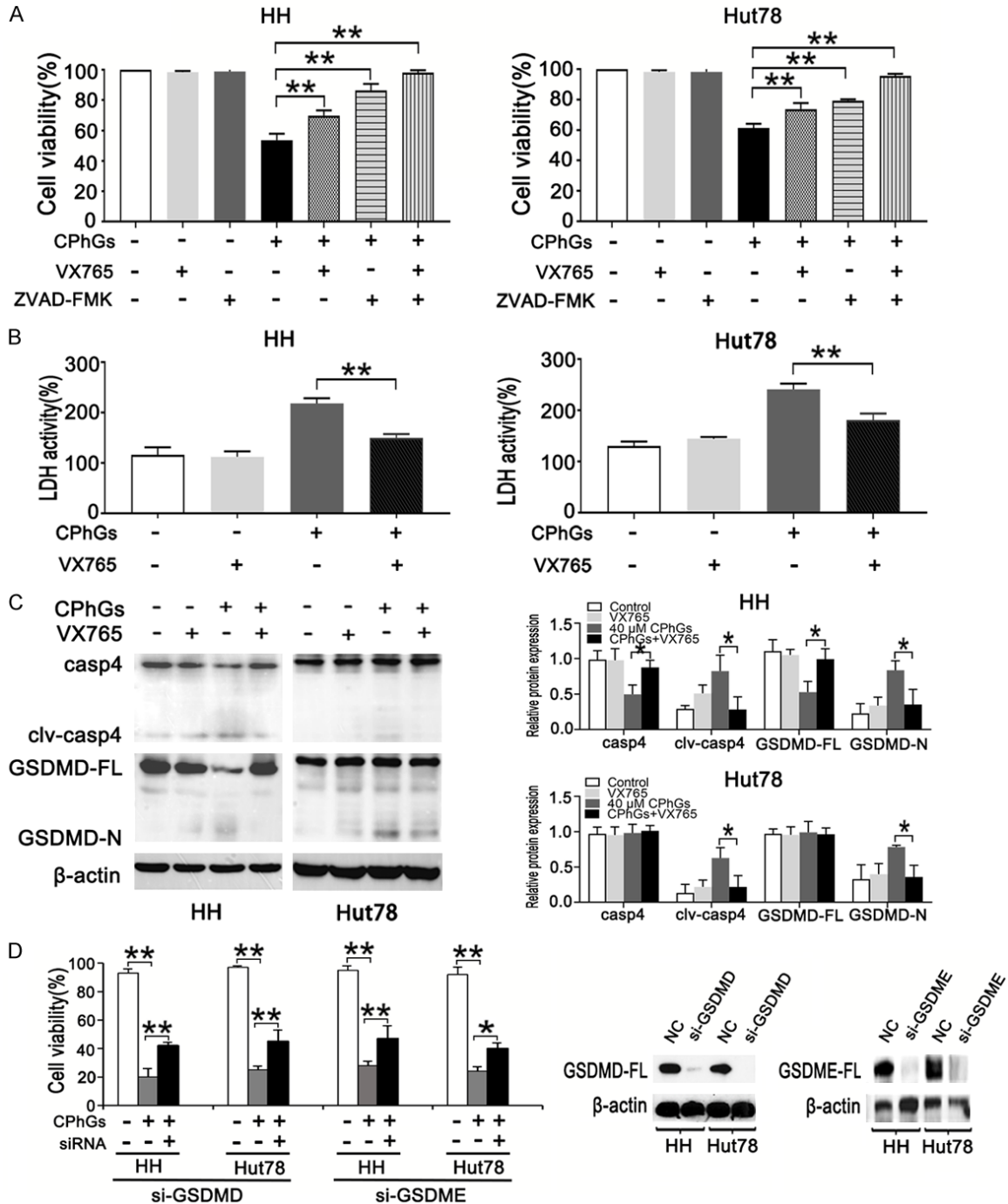
Figure 4. CPhGs activated non-canonical and alternative pyroptotic pathways but not the canonical pyroptotic pathway. Cells were pre-treated with 20 μM ZVAD-FMK or/and VX765 followed by indicated concentrations of CPhGs. A. Cell survival rates following treatment. B. Changes in LDH levels. C. Western blotting results for specified proteins. D. Cells transfected with specified siRNAs, and the effects of GSDMD/E knockdown on cell viability were assessed (left). Western blot showing silencing effects of siRNAs (right). White, gray, and black columns represent control, CPhGs, and CPhGs+GSDMD/E siRNAs, respectively. Data are represented as the mean ± SD. **$P < 0.01$ compared to CPhGs only.

Studies on single or a mixture of multiple CPhGs have revealed that their anti-cancer mechanisms include the induction of apoptosis by regulating multiple signaling pathways [10, 11, 22]. In the present study, CPhGs triggered both intrinsic and extrinsic apoptosis. Pro-apoptosis
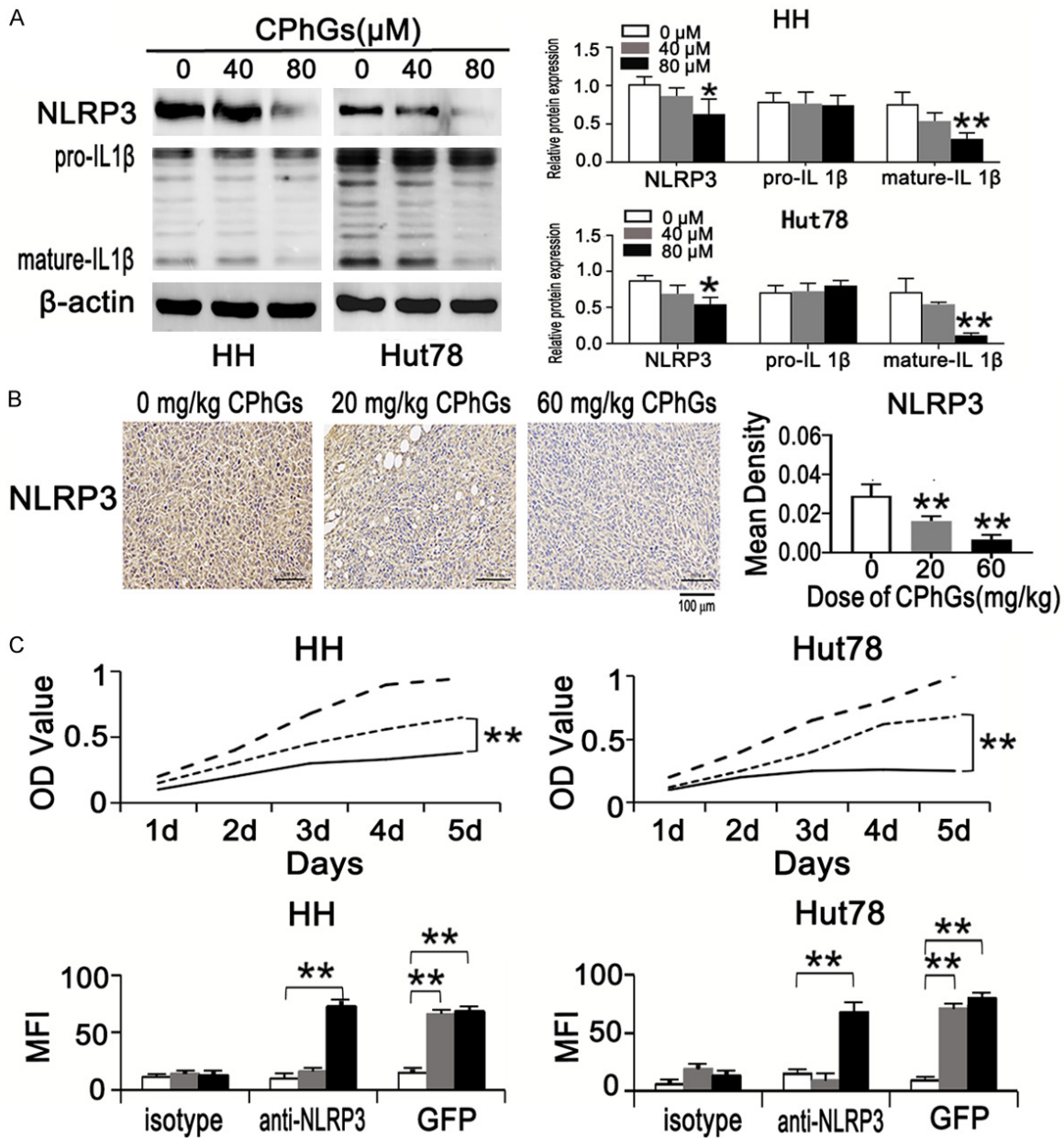
Figure 5. CPhGs inhibited the expression of NLRP3 and maturation of IL-1β. HH and Hut78 cells were treated with CPhGs. A. The expression of NLRP3, pro-IL-1β, and matured IL-1β were detected by Western Blotting. Quantitative results are displayed by histograms. B. Representative images of NLRP3-specific immunohistochemical staining of xenograft tumor tissues with results quantified by histograms. C. Upper panel: Rescue effect of forced expression of NLRP3 on cell death. The long dotted line, solid line, and short dotted lines represent the non-treatment group, CPhGs treated group and CPhGs-treated + NLRP3 forced expression group, respectively. Lower panel: The transfection and expression efficiencies of forced expression of NLRP3 by pcDNA3.1-GFP plasmid transfection. X-axis shows isotype antibody, anti-NLRP3 antibody, and GFP signals. White, gray, and black columns indicate untransfected, empty vector-transfected, and NLRP3 vector-transfected cells respectively. Data are presented as mean ± SD and compared control group, *P < 0.05, **P < 0.01. Scale: 100 μm.

factors such as P53, PTEN, and BAX were upregulated, whereas anti-apoptosis factors including Bcl-2, PI3K, and AKT were inhibited, suggesting that the anti-cancer function of CPhGs is derived through regulating these

pathways. Silent information regulator 2 (SIRT2) is a histone deacetylase that regulates multiple cellular functions including cell cycle, proliferation, and apoptosis [23]. The role of SIRT2 in malignant cells remains unclear. It may func-
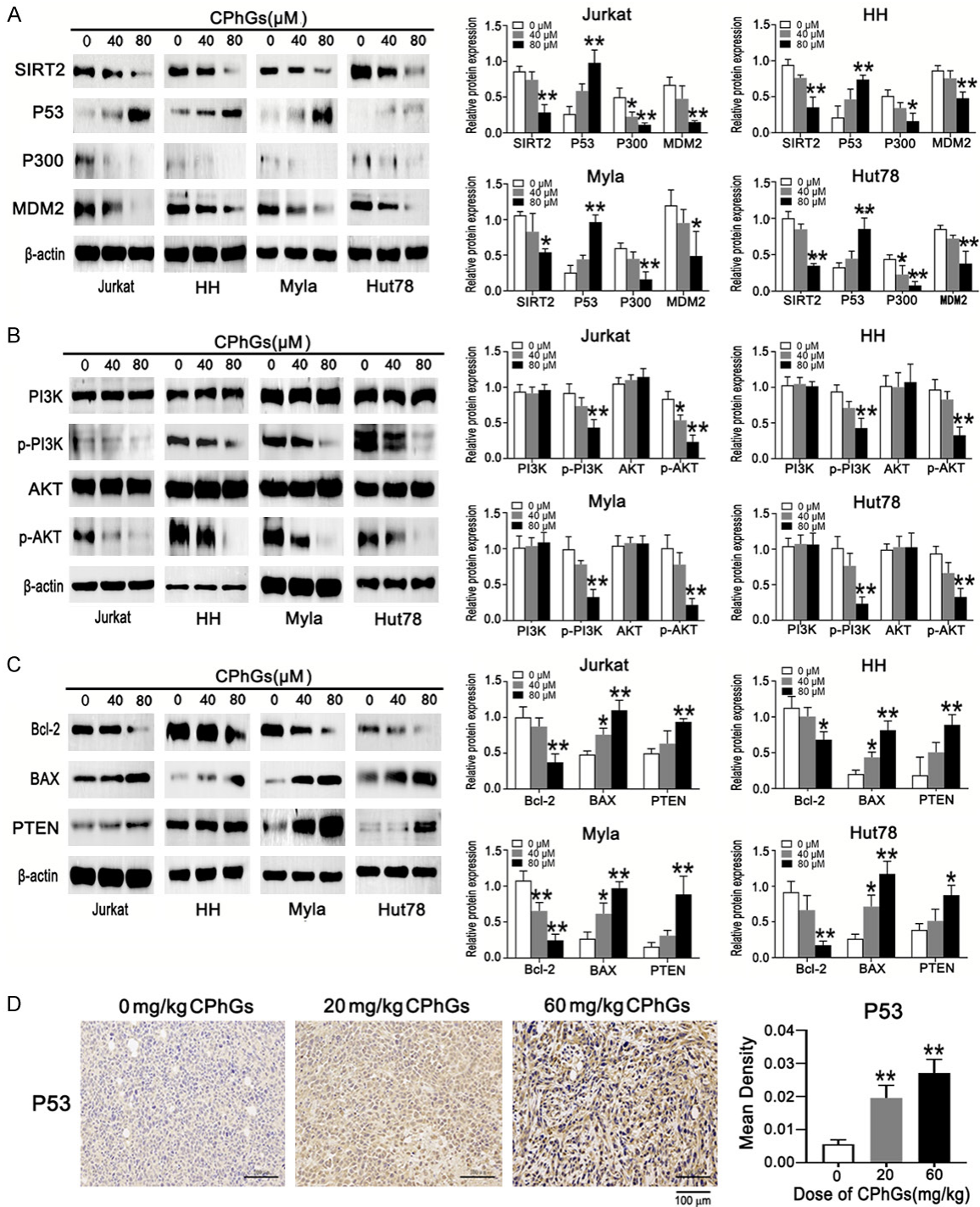
Figure 6. CPhGs modulate multiple cellular signaling pathways contributing to apoptosis. (A-C) Western blotting detection of the expression of key proteins in the SIRT2/P53 (A), PI3K/AKT (B), and pro-/anti-apoptosis pathways (C). (D) Representative images of P53-specific immunohistochemical staining of xenograft tumor tissues, with data quantified by histogram (right). Data are presented as mean ± SD. *P < 0.05, **P < 0.01. Scale: 100 μm.

tion as either a tumor suppressor or oncogenic factor, depending on cell type and physiological conditions, by influencing downstream proteins such as P53, P300, NF-kB, and MDM2 (murine double minute 2) [24]. P53 is a tumor-suppressor gene that can be negatively regulated by its upstream SIRT2-P300/MDM2 signal axis [24, 25]. In addition, evidence shows that PI3K/AKT
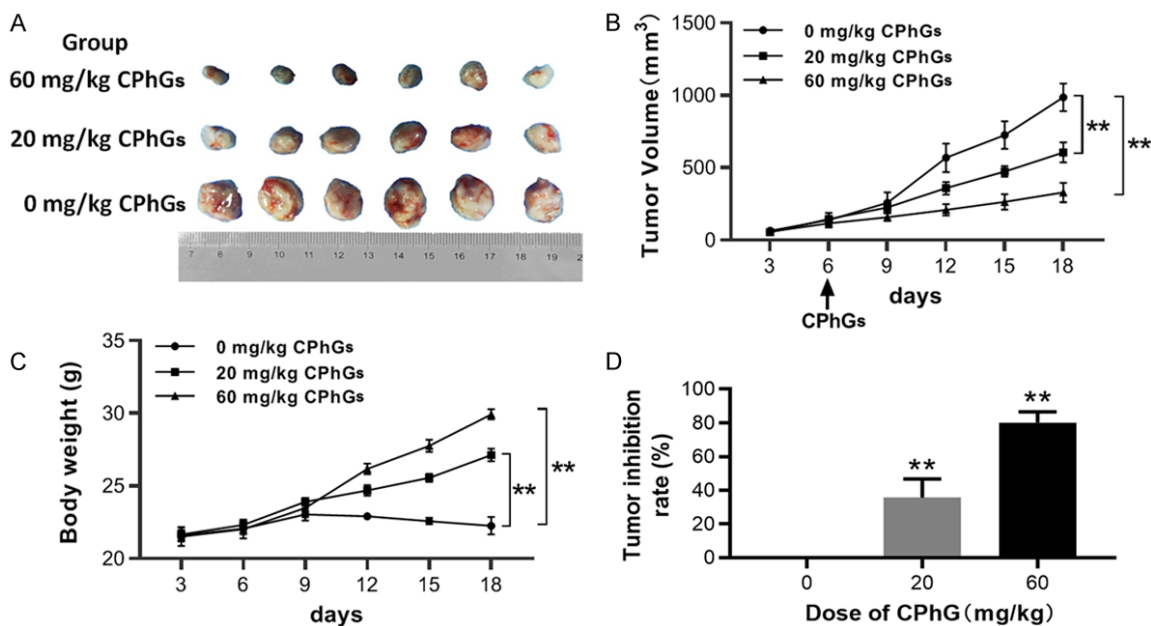
Figure 7. CPhGs inhibited tumor growth in a xenograft TCL mouse model. A. Image representing tumors surgically dissected from six groups of mice (columns 1-6) treated with doses of 0, 20, and 60 CPhGs (mg/kg body weight). B. Tumor growth curves plotted at the end of the observation period (18 d). C. Body weight changes of mice over 18 d. D. Tumor inhibition rates were calculated using the formula: (mean tumor weight of the control group - treatment group)/control group * 100%.

signaling enhances MDM2 expression, which targets P53 for degradation [26]. In this study, P53 up-regulation was accompanied by the inhibition of the SIRT2-P300/MDM2 axes and PI3K/AKT signaling. Therefore, CPhGs positively modulate P53 by directly and indirectly blocking SIRT2-P300/MDM2 axes. The proposed mechanisms of CPhGs-induced apoptosis are summarized in **Figure 8** (left section).

The activation of pyroptosis can be summarized in three pathways: 1. the canonical pathway which encompasses the sequential steps of NLRP3 inflammasome formation, caspase-1 activation, and cleavage of Gasdermin D (GSDMD); 2. the non-canonical pyroptotic pathway, with activation of caspase-4/5/11 and GSDMD cleavage; and 3. an alternative pathway, mediated by caspase-3 and Gasdermin E (GSDME). Given the caspase-3 is also the executor of apoptosis it serves as a key component of both the apoptosis and pyroptosis pathways, facilitating the switch between apoptosis-pyroptosis under certain conditions. The cleaved N-terminal fragments of GSDMD and GSDME (GSDMD-N and GSDME-N), acting as executive proteins of pyroptosis, form pores in the cell membrane, leading to K+ efflux, H_2O

influx, and subsequent osmotic cell swelling and death [18, 27, 28].

The role of CPhGs-induced pyroptosis in disease treatment remains controversial. CPhGs have demonstrated the ability to either trigger or inhibit pyroptosis, depending on the disease or cell type. For example, echinacoside, a principal component of the CPhGs family, induces pyroptosis in lung cancer cells through mitochondria-mediated Raf/MEK/ERK signaling, yet inhibits pyroptosis in cardiomyocytes and neurons in non-cancer diseases [17, 29, 30]. Thus, pyroptosis may be beneficial or detrimental, contingent on the tissue or disease context. In this study, we determined that CPhGs induced significant pyroptosis, exerting a synergistic cytotoxic effect alongside apoptosis in malignant T cells.

Additionally, related signaling pathways may exhibit dual effects, even within the context of cancer treatment alone. The NLRP3 inflammasome, a complex comprising NLRP3, ASC, and caspase-1, plays a pivotal role in the canonical pyroptotic pathway. However, the NLRP3 inflammasome also promotes tumor proliferation, metastasis, and invasion through cas-
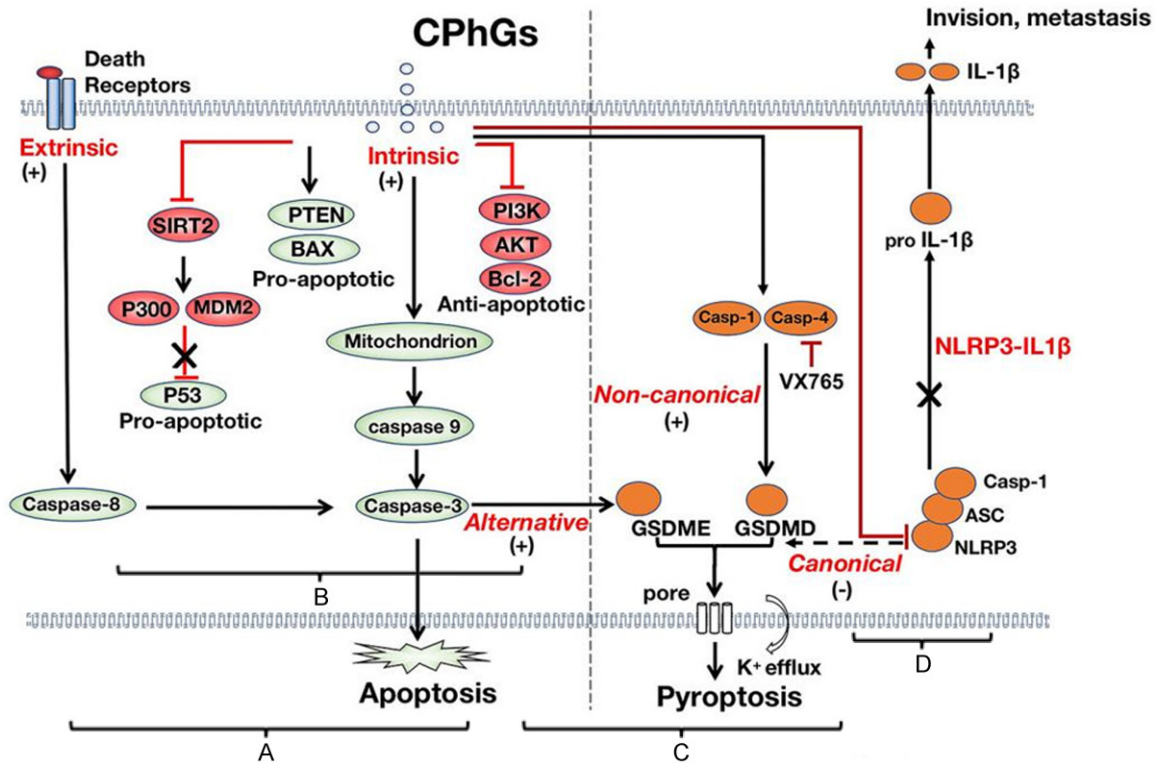
Figure 8. The molecular mechanisms of the anti-tumor properties of CPhGs. A schematic figure illustrates that CPhGs: A. Induce apoptosis by activating both intrinsic and extrinsic apoptotic pathways; B. Up-regulate pro-apoptotic factors PTEN and BAX, increase tumor-suppressor P53 by inhibiting SIRT2/MDM2 signaling, and suppress anti-apoptotic PI3K/AKT signaling; C. Induce pyroptosis by activating both caspase-4 (non-canonical pyroptosis) and caspase-3 (alternative pyroptosis) pathways; D. Inhibit proliferation by down-regulating NLRP3 and downstream IL-1β. Red lines denote inhibitory effects, and 'x' indicates blockade of functions. Italicized text in red shows three pyroptosis pathways. (+) and (-) denote activation and non-activation of the pathways, respectively. The figure is divided into two parts by a dotted line in the middle. The left part outlines the key components of apoptosis and their relationships. Both caspase-8 and -9 are activated to cleave the executor caspase-3, resulting in apoptosis and possibly an apoptosis-pyroptosis switch. The right part shows the mechanism of pyroptosis: GSDMD and GSDME are pyroptosis executors that form pores in the cell membrane, leading to K+ efflux, cell swelling, and death. VX765 is identified as a caspase 4 inhibitor, blocking non-canonical pyroptosis.

pase-1 mediated maturation of IL-1β [31]. Studies have shown that inhibition of NLRP3 leads to the regression of cancer cells both *in vitro* and *in vivo* [32-35]. Consequently, activating NLRP3 inflammasome signaling represents a "double-edged sword" in cancer therapy, beneficial for inducing pyroptosis in cancer cells but potentially contributing to cancer pathogenesis. Since agents that induce pyroptosis via the canonical pathway will inevitably activate NLRP3 inflammasome signaling, identifying agents that can separately modulate pyroptosis and NLRP3 inflammasome signaling will emerge as valuable drug candidates for achieving optimal anti-cancer effects. In this study, CPhGs effectively induced pyroptosis by activating caspase-4 and -5 as well as cas-

pase-3 signaling, but not caspase-1 signaling. Conversely, CPhGs down regulated NLRP3 expression and inhibited NLRP3/caspase-1 inflammasome signaling and subsequent IL-1β maturation. Therefore, CPhGs simultaneously promotes pyroptosis and inhibits IL-1β-driven proliferation.

Caspase-3, known as an apoptosis executor, may also play a crucial role in alternative pyroptotic signaling by cleaving GSDME. Like GSDMD, GSDME, a gasdermin superfamily member, facilitates pore formation in the cell membrane. Activated caspase-3 can initiate pyroptosis, transitioning the cell death type from apoptosis to pyroptosis [36, 37]. Given the activation of GSDME in our findings, caspase-3

acts as a central junction of the two cell death pathways, inducing both apoptosis and pyroptosis in CPhGs-treated malignant T cells. The proposed mechanisms of CPhGs-induced pyroptosis and NLRP3 and IL-1β inhibition are shown in the right section of schematic **Figure 8**.

P53 plays a comprehensive role in cellular functions and contributes to the activation of NLRP3 and caspase-1 [38]. However, our data showed that elevated P53 doses did not correlate with the activation of NLRP3/caspase-1 by CPhGs treatment. Numerous studies have demonstrated that P53 promotes caspase-3 activation. Therefore, P53 can engage in pyroptosis by supporting the caspase-3-GSDME dependent alternative pyroptotic pathway. Similarly, inhibition of PI3K/AKT and increased levels of PTEN and BAX can elevate caspase-3 levels, thereby triggering both pyroptosis and apoptosis.

As stated above, our research utilized a mixture of four CPhGs to investigate the integrated function of the herb *C. deserticola*. While further research is necessary to elucidate each function of CPhGs, at this study stage, we have determined that CPhGs induce apoptosis and pyroptosis by modulating multiple signaling pathways, significantly inhibiting TCL growth *in vitro* and *in vivo*. We reveal a novel mechanism that CPhGs plays dual functions in promoting pyroptosis and inhibiting IL-1β dependent proliferation. As summarized in **Figure 8**, CPhGs comprehensively influence the network of intrinsic and extrinsic apoptotic pathways, noncanonical and alternative pyroptotic pathways, tumor-suppressing and -promoting pathways, along with their interactions. Our study suggests that CPhGs may be effective for the treatment of TCL.

Acknowledgements

Disclosure of conflict of interest

None.

Abbreviations

TCL, T-cell lymphoma; TCM, Traditional Chinese Medicine; *C. deserticola*, Cistanche deserticola Y. C. Ma; CPhGs, Cistanche-derived phenylethanoid glycosides; SIRT2, Silent information regulatory 2; BAX, BCL-2 Associated X; Bcl-2, B-cell lymphoma-2; MDM2, Murine double minute 2; PTEN, Phosphatase and tensin homolog deleted on chromosome ten; GSDMD, Gasdermin D; GSDME, Gasdermin E; NLRP3, NOD-, LRR- and pyrin domain-containing protein 3; PBS, Phosphate-buffered saline; CCK8, Cell Counting Kit-8; OD, Optical density; mRNA, Messenger RNA; PI, Propidium Iodide; RT-PCR, Real-time Polymerase chain reaction; SDS-PAGE, Sodium dodecyl sulfate polyacrylamide gel electrophoresis; HE, Hematoxylin-Eosin.

Address correspondence to: Jianqiang Wu and Hongxin Yang, College of Basic Medicine, Inner Mongolia Medical University, Hohhot, Inner Mongolia, China. Tel: +86-0471-4993164; E-mail: jianqiangwu@immu.edu.cn (JQW); Tel: +86-0471-6636217; E-mail: hongxinyang@immu.edu.cn (HXY)

References

[1] Liu Y, Yang S, Wang K, Lu J, Bao X, Wang R, Qiu Y, Wang T and Yu H. Cellular senescence and cancer: focusing on traditional Chinese medicine and natural products. Cell Prolif 2020; 53: e12894.

[2] Wang T, Zhang X and Xie W. Cistanche deserticola Y. C. Ma, "Desert ginseng": a review. Am J Chin Med 2012; 40: 1123-1141.

[3] Zhou S, Feng D, Zhou Y, Duan H, Jiang Y and Yan W. Analysis of the active ingredients and health applications of cistanche. Front Nutr 2023; 10: 1101182.

[4] Liao PL, Li CH, Tse LS, Kang JJ and Cheng YW. Safety assessment of the Cistanche tubulosa health food product Memoregain® : genotoxicity and 28-day repeated dose toxicity test. Food Chem Toxicol 2018; 118: 581-588.

[5] Xiang L, Mei X, Luo H, Wang S, Wang X and Jiao W. Comparison of phenylethanolic glycosides in different species, producing area and growing period of Cistanche herb. Food Industry 2022; 43: 124-129.

[6] Ma X, Dong Y, Guo Q and Ding H. Determination of six phenylethanoid glycosides in Cistanche tubulosa and Cistanche deserticola by QAMS. Lishizhen Medicine and Materia Medica Research 2018; 29: 2309-2312.

[7] Zhang H, Xiang Z, Duan X, Jiang JL, Xing YM, Zhu C, Song Q and Yu QR. Antitumor and anti-inflammatory effects of oligosaccharides from Cistanche deserticola extract on spinal cord injury. Int J Biol Macromol 2019; 124: 360-367.

[8] Yuan P, Li J, Aipire A, Yang Y, Xia L, Wang X, Li Y and Li J. Cistanche tubulosa phenylethanoid glycosides induce apoptosis in H22 hepatocellular carcinoma cells through both extrinsic and intrinsic signaling pathways. BMC Complement Altern Med 2018; 18: 275.

[9] Yuan P, Fu C, Yang Y, Adila A, Zhou F, Wei X, Wang W, Lv J, Li Y, Xia L and Li J. Cistanche tubulosa phenylethanoid glycosides induce apoptosis of hepatocellular carcinoma cells by mitochondria-dependent and MAPK pathways and enhance antitumor effect through combination with cisplatin. Integr Cancer Ther 2021; 20: 15347354211013085.

[10] Tang C, Gong L, Lvzi X, Qiu K, Zhang Z and Wan L. Echinacoside inhibits breast cancer cells by suppressing the Wnt/beta-catenin signaling pathway. Biochem Biophys Res Commun 2020; 526: 170-175.

[11] Liu J, Tang N, Liu N, Lei P and Wang F. Echinacoside inhibits the proliferation, migration, invasion and angiogenesis of ovarian cancer cells through PI3K/AKT pathway. J Mol Histol 2022; 53: 493-502.

[12] Li W, Zhou J, Zhang Y, Zhang J, Li X, Yan Q, Han J and Hu F. Echinacoside exerts anti-tumor activity via the miR-503-3p/TGF-beta1/Smad aixs in liver cancer. Cancer Cell Int 2021; 21: 304.

[13] Shi S, Qin Y, Chen D, Deng Y, Yin J, Liu S, Yu H, Huang H, Chen C, Wu Y, Zou D and Wang Z. Echinacoside (ECH) suppresses proliferation, migration, and invasion of human glioblastoma cells by inhibiting Skp2-triggered epithelial-mesenchymal transition (EMT). Eur J Pharmacol 2022; 932: 175176.

[14] Wang W, Luo J, Liang Y and Li X. Echinacoside suppresses pancreatic adenocarcinoma cell growth by inducing apoptosis via the mitogen-activated protein kinase pathway. Mol Med Rep 2016; 13: 2613-2618.

[15] Ye Y, Song Y, Zhuang J, Wang G, Ni J and Xia W. Anticancer effects of echinacoside in hepatocellular carcinoma mouse model and HepG2 cells. J Cell Physiol 2019; 234: 1880-1888.

[16] Li J, Li J, Aipire A, Gao L, Huo S, Luo J and Zhang F. Phenylethanoid glycosides from Cistanche tubulosa inhibits the growth of B16-F10 cells both in vitro and in vivo by induction of apoptosis via mitochondria-dependent pathway. J Cancer 2016; 7: 1877-1887.

[17] Shi Y, Cao H, Liu Z, Xi L and Dong C. Echinacoside induces mitochondria-mediated pyropto-sis through Raf/MEK/ERK signaling in non-small cell lung cancer cells. J Immunol Res 2022; 2022: 3351268.

[18] Fang Y, Tian S, Pan Y, Li W, Wang Q, Tang Y, Yu T, Wu X, Shi Y, Ma P and Shu Y. Pyroptosis: a new frontier in cancer. Biomed Pharmacother 2020; 121: 109595.

[19] Wu J, Nihal M, Siddiqui J, Vonderheid EC and Wood GS. Low FAS/CD95 expression by CTCL correlates with reduced sensitivity to apoptosis that can be restored by FAS upregulation. J Invest Dermatol 2009; 129: 1165-1173.

[20] Wu J and Wood GS. Reduction of Fas/CD95 promoter methylation, upregulation of Fas protein, and enhancement of sensitivity to apoptosis in cutaneous T-cell lymphoma. Arch Dermatol 2011; 147: 443-449.

[21] Wang L, Zhou GB, Liu P, Song JH, Liang Y, Yan XJ, Xu F, Wang BS, Mao JH, Shen ZX, Chen SJ and Chen Z. Dissection of mechanisms of Chinese medicinal formula Realgar-Indigo naturalis as an effective treatment for promyelocytic leukemia. Proc Natl Acad Sci U S A 2008; 105: 4826-4831.

[22] Dong L, Yu D, Wu N, Wang H, Niu J, Wang Y and Zou Z. Echinacoside induces apoptosis in human SW480 colorectal cancer cells by induction of oxidative DNA damages. Int J Mol Sci 2015; 16: 14655-14668.

[23] Li C, Zhou Y, Rychahou P, Weiss HL, Lee EY, Perry CL, Barrett TA, Wang Q and Evers BM. SIRT2 contributes to the regulation of intestinal cell proliferation and differentiation. Cell Mol Gastroenterol Hepatol 2020; 10: 43-57.

[24] Bosch-Presegue L and Vaquero A. The dual role of sirtuins in cancer. Genes Cancer 2011; 2: 648-662.

[25] Li Y, Matsumori H, Nakayama Y, Osaki M, Kojima H, Kurimasa A, Ito H, Mori S, Katoh M, Oshimura M and Inoue T. SIRT2 down-regulation in HeLa can induce p53 accumulation via p38 MAPK activation-dependent p300 decrease, eventually leading to apoptosis. Genes Cells 2011; 16: 34-45.

[26] Abraham AG and O'Neill E. PI3K/Akt-mediated regulation of p53 in cancer. Biochem Soc Trans 2014; 42: 798-803.

[27] Xia X, Wang X, Cheng Z, Qin W, Lei L, Jiang J and Hu J. The role of pyroptosis in cancer: pro-cancer or pro-"host"? Cell Death Dis 2019; 10: 650.

[28] Sun Q and Scott MJ. Caspase-1 as a multifunctional inflammatory mediator: noncytokine maturation roles. J Leukoc Biol 2016; 100: 961-967.

[29] Ni Y, Zhang J, Zhu W, Duan Y, Bai H and Luan C. Echinacoside inhibited cardiomyocyte pyroptosis and improved heart function of HF rats induced by isoproterenol via suppressing

NADPH/ROS/ER stress. J Cell Mol Med 2022; 26: 5414-5425.

[30] Gao MR, Wang M, Jia YY, Tian DD, Liu A, Wang WJ, Yang L, Chen JY, Yang Q, Liu R and Wu YM. Echinacoside protects dopaminergic neurons by inhibiting NLRP3/Caspase-1/IL-1beta signaling pathway in MPTP-induced Parkinson's disease model. Brain Res Bull 2020; 164: 55-64.

[31] Zhai Z, Liu W, Kaur M, Luo Y, Domenico J, Samson JM, Shellman YG, Norris DA, Dinarello CA, Spritz RA and Fujita M. NLRP1 promotes tumor growth by enhancing inflammasome activation and suppressing apoptosis in metastatic melanoma. Oncogene 2017; 36: 3820-3830.

[32] Fan SH, Wang YY, Lu J, Zheng YL, Wu DM, Li MQ, Hu B, Zhang ZF, Cheng W and Shan Q. Luteoloside suppresses proliferation and metastasis of hepatocellular carcinoma cells by inhibition of NLRP3 inflammasome. PLoS One 2014; 9: e89961.

[33] Chow MT, Sceneay J, Paget C, Wong CS, Duret H, Tschopp J, Moller A and Smyth MJ. NLRP3 suppresses NK cell-mediated responses to carcinogen-induced tumors and metastases. Cancer Res 2012; 72: 5721-5732.

[34] Sharma BR and Kanneganti TD. NLRP3 inflammasome in cancer and metabolic diseases. Nat Immunol 2021; 22: 550-559.

[35] Hamarsheh S and Zeiser R. NLRP3 inflammasome activation in cancer: a double-edged sword. Front Immunol 2020; 11: 1444.

[36] Wang Y, Gao W, Shi X, Ding J, Liu W, He H, Wang K and Shao F. Chemotherapy drugs induce pyroptosis through caspase-3 cleavage of a gasdermin. Nature 2017; 547: 99-103.

[37] Huang Y, Xu W and Zhou R. NLRP3 inflammasome activation and cell death. Cell Mol Immunol 2021; 18: 2114-2127.

[38] Ranjan A and Iwakuma T. Non-canonical cell death induced by p53. Int J Mol Sci 2016; 17: 2068.